007, 2022,

from https://agupubs.onlinelibrary.wiley.com/doi/10.1029/2022GL099583 by University Of Montana Mansfield Library-Serials, Wiley Online Library on [02/12/2022]. See the Terms and Conditions (https://agupubs.onlinelibrary.wiley.com/doi/10.1029/2022GL099583 by University Of Montana Mansfield Library-Serials, Wiley Online Library on [02/12/2022]. See the Terms and Conditions (https://agupubs.onlinelibrary.wiley.com/doi/10.1029/2022GL099583 by University Of Montana Mansfield Library-Serials, Wiley Online Library on [02/12/2022]. See the Terms and Conditions (https://agupubs.onlinelibrary.wiley.com/doi/10.1029/2022GL099583 by University Of Montana Mansfield Library-Serials, Wiley Online Library on [02/12/2022]. See the Terms and Conditions (https://agupubs.onlinelibrary.wiley.com/doi/10.1029/2022GL099583 by University Of Montana Mansfield Library-Serials, Wiley Online Library on [02/12/2022].



# **Geophysical Research Letters**°

# RESEARCH LETTER

10.1029/2022GL099583

#### **Key Points:**

- The seasonal oscillation in mountain groundwater is 1/5 of yearly cumulative precipitation and 1/2 of the oscillation in total water storage
- The southern Central Valley has lost groundwater at 1.5 ± 0.4 km³/yr since 2006, accounting for 68% of the total loss in the Valley
- 50 km³ of water enters the Central Valley each year; 56% is river water, 34% precipitation, and 10% groundwater (mountain-block recharge)

#### **Supporting Information:**

Supporting Information may be found in the online version of this article.

#### Correspondence to:

D. F. Argus, donald.f.argus@jpl.nasa.gov

#### Citation:

Argus, D. F., Martens, H. R., Borsa, A. A., Knappe, E., Wiese, D. N., Alam, S., et al. (2022). Subsurface water fluxin California's Central Valley and its source watershed from space geodesy. *Geophysical Research Letters*, 49, e2022GL099583. https://doi.org/10.1029/2022GL099583

Received 25 MAY 2022 Accepted 13 SEP 2022

#### © 2022 American Geophysical Union. All Rights Reserved. California Institute of Technology. Government sponsorship acknowledged.

# **Subsurface Water Flux in California's Central Valley and Its Source Watershed From Space Geodesy**

Donald F. Argus<sup>1</sup>, Hilary R. Martens<sup>2</sup>, Adrian A. Borsa<sup>3</sup>, Ellen Knappe<sup>3</sup>, David N. Wiese<sup>1</sup>, Sarfaraz Alam<sup>4</sup>, Mackenzie Anderson<sup>5</sup>, Ashlesha Khatiwada<sup>2</sup>, Nicholas Lau<sup>3</sup>, Athina Peidou<sup>1</sup>, Matthew Swarr<sup>2</sup>, Alissa M. White<sup>2</sup>, Machiel S. Bos<sup>6</sup>, Matthias Ellmer<sup>1</sup>, Felix W. Landerer<sup>1</sup>, and W. Payton Gardiner<sup>2</sup>

<sup>1</sup>Jet Propulsion Laboratory, California Institute of Technology, Pasadena, CA, USA, <sup>2</sup>University of Montana, Missoula, MT, USA, <sup>3</sup>Scripps Institution of Oceanography, University of California San Diego, La Jolla, CA, USA, <sup>4</sup>Stanford University, Stanford, CA, USA, <sup>5</sup>University of California Los Angeles, Los Angeles, CA, USA, <sup>6</sup>University of Porto, Porto, Portugal

**Abstract** We integrate Global Positioning System displacements, Gravity Recovery and Climate Experiment gravity data, reservoir water volumes, and snowpack to estimate change in subsurface water in California. We find 29% of precipitation infiltrates mountain soil and fractured bedrock each autumn and winter and is lost in the spring and summer by evapotranspiration and lateral subsurface flow either within mountain watersheds or into California's Central Valley. The Central Valley lost groundwater at  $2.2 \pm 0.7 \text{ km}^3/\text{yr}$  from 2006 to 2021, with 68% of the loss occurring in the southern third of the Valley. Water in Central Valley fluctuates each year by a mean of  $10.7 \pm 1.1 \text{ km}^3$  with maximum water in April (not August). A third of Central Valley groundwater lost during recent severe drought is recharged during subsequent years of heavy precipitation. Of the 50 km³ of water entering Central Valley each year, 28 km³ comes from rivers, 17 km³ from precipitation, and 5 km³ from mountain groundwater.

**Plain Language Summary** We combine measurements from Global Positioning System positioning and Gravity Recovery and Climate Experiment gravity to infer change in water components in Central Valley and its source watershed, the Sacramento-San Joaquin-Tulare River basin better than possible with either technique separately. We find that the Central Valley has lost groundwater from 2006 to 2021 at  $2.2 \pm 0.7$  km<sup>3</sup>/yr (95% confidence limits follow the " $\pm$ " sign), with 2/3 of the groundwater loss occurring in the southern part of the Valley. We estimate the seasonal recharge and loss of subsurface water in the Central Valley. Comparison to a model accounting for precipitation, evapotranspiration, and river water entering and leaving the Central Valley suggests that deep groundwater may be flowing from the Sierra Nevada mountains into the Central Valley.

#### 1. Introduction

#### 1.1. Drought and Heavy Precipitation

El Niño and La Niña produce alternating periods of drought and years of heavy precipitation in California (Cayan et al., 1999) (Figure S1 in Supporting Information S1). Anthropogenic greenhouse gases have warmed Earth by 0.9°C since 1950, creating harsher droughts and fiercer flooding in the west U.S. (IPCC, 2021). Severe drought struck California from October 2011 to October 2015 (Griffin & Anchukaitis, 2014; Swain et al., 2014). Precipitation was low and temperature high during the 4 years (PRISM Climate Group, 2017). Snow accumulation in the Sierra Nevada in the winters of 2014 and 2015 was less than 1/4 of its average (NOHRSC, 2004), resulting in a shortfall of freshwater available for agriculture and urban centers.

Heavy precipitation replenished water in California from October 2015 to October 2019. In water years 2017 and 2019, 14 and 6 major atmospheric rivers, respectively, brought heavy rain and snow to the Sacramento-San Joaquin-Tulare (SST) River basin (CDWR, 2018), resulting in maximum snowpack in the Sierra Nevada of 27 and 37 km³, nearly twice the average from 2006 to 2021 (NOHRSC, 2004) (Figure 1 and Figure S1 in Supporting Information S1). Since October 2019, drought has again struck the southwest U.S. In water year 2021, precipitation was half its historical average and temperatures were high, resulting in extreme drought in the autumn of 2021 (U.S. Drought Monitor, 2021) and bringing surface water in artificial reservoirs to historic lows.

ARGUS ET AL. 1 of 12

Wiley Online Library on [02/12/2022]. See the Terms

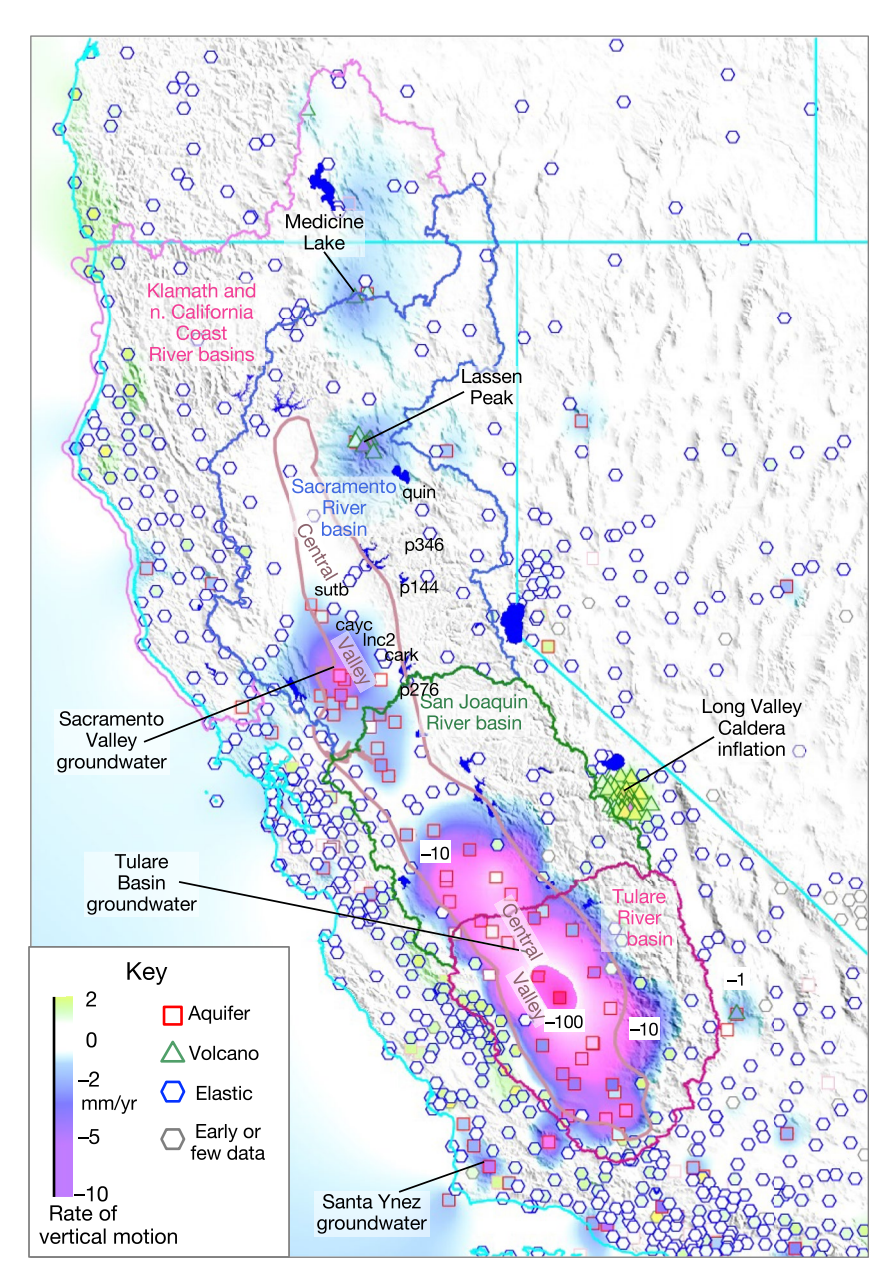


**Figure 1.** River watersheds (outlined in various colors), mean rate of vertical motion from January 2006 to December 2021, and GPS sites (symbols). This study focuses on the Sacramento (blue), San Joaquin (green), and Tulare River (violet red) watersheds. The Klamath and north California Coast River watershed (pink) is also plotted. Color gradations depict nearly zero vertical motion (white color), slow uplift (light green), slow subsidence (light blue), and fast subsidence (magenta). See legend at bottom left for vertical rates. Contours of vertical motion at 10 mm/yr (violet to magenta) and 100 mm/yr in the southern Central Valley are labeled. The shape of the symbol at each GPS site designates the primary phenomenon deforming solid Earth at the site: porous response to groundwater change (red squares), elastic response to water oscillations (blue hexagons), and volcanic activity (green triangles). Early data before 2006 (gray circles) are omitted. The hexagons are filled with the color designating vertical motion in mm/yr observed at the GPS site (see legend). River basins are Hydrologic Unit Code 4 watersheds from the National Hydrography Data set (https://www.usgs.gov/national-hydrography/national-hydrography-dataset). The Central Valley is a physiographic province (Thelin & Pike, 1991).

NASA missions are allowing technologists and scientists to estimate change in total water storage in the context of megadrought reducing the availability of freshwater resources (Landerer et al., 2020). The Global Positioning System (GPS) has emerged as a valuable technique to infer change in total water at Earth's surface using measurements of solid Earth's elastic response to mass change (Borsa et al., 2014; Argus, Fu, & Landerer, 2014),

ARGUS ET AL. 2 of 12

thereby complementing Gravity Recovery and Climate Experiment (GRACE) data. In this study, we (a) integrate GPS and GRACE to estimate change in total water as a function of location each month from January 2006 to May 2022, thus adding GRACE to and updating the water series of Argus et al. (2017); (b) quantify change in total water storage and its partitioning among river basins (Figure 1) and physiographic provinces (Figure S2 in Supporting Information S1) in the western U.S.; and (c) infer change in bedrock groundwater by removing a composite model consisting of snow water equivalent and soil moisture from total water inferred from GPS and GRACE.

#### 1.2. Central Valley Groundwater Recharge and Pumping

The Central Valley, California, produces 1/12 of the United States' agricultural output in dollars and a quarter of the nation's food (Faunt, 2009). Water for agriculture comes primarily from precipitation and rivers draining the mountains surrounding the Valley. Water is stored as snowpack in the Sierra Nevada and in artificial reservoirs along rivers bringing water from the mountains to the Valley. Extensive infrastructure, consisting of dams, aqueducts, and canals, provides water to irrigate the crops. In dry years, farmers pump groundwater from the Central Valley aquifer to irrigate agricultural areas. Anthropogenic pumping has caused parts of the Central Valley to sink as much as 3 m since 1962 in response to a total net loss of 100 km<sup>3</sup> of groundwater (Faunt, 2009; Figure C21, Faunt et al., 2015; Figure 2, Scanlon et al., 2012).

Famiglietti et al. (2011) estimate change in groundwater in the Central Valley using GRACE and the Global Land Data Assimilation System model (Rodell et al., 2004). Several studies (Ahamed et al., 2022; Alam et al., 2021; Liu et al., 2019; Kim et al., 2020; Ojha et al., 2018, 2019) have followed Famiglietti et al.'s seminal formulation. GRACE resolves change in total water storage at a spatial resolution of about 330 km, less than the 500-km altitude of the two GRACE satellites. GRACE can determine change in total water in the large SST River basin, with an area of 154,800 km²; but not in the small Central Valley, with an area of 48,800 km².

Famiglietti et al. (2011) infer change in Central Valley groundwater assuming change in mountain groundwater to be negligible:

$$\Delta CV_{groundwater} = \Delta SST_{GRACE} - \Delta SST_{surface water} - \Delta SST_{snow} - \Delta SST_{soil moisture}$$
(1)

where  $\Delta SST_{GRACE}$  is change in total water in the SST River basin from GRACE,  $\Delta SST_{surface\ water}$  is known change in artificial reservoir surface water, and  $\Delta SST_{snow}$  and  $\Delta SST_{soil\ moisture}$  are change in snow and soil moisture in a land surface hydrology model. However, seasonal oscillations and interannual fluctuations in subsurface water differ significantly from those assumed in the hydrology models, as evident in Argus et al. (2017) estimates of changes in total water from the elastic rise and fall of the Sierra Nevada, Cascade mountains, Klamath mountains, and Coast Ranges. In this study, we estimate change in groundwater in the Central Valley by integrating GPS elastic displacements and GRACE gravity observations. The dense array of GPS sites in the Pacific Mountain system constrain change in total water in all the mountain provinces and in the northern Central Valley, but not in the southern Central Valley, where GPS sites record primarily the porous response of the aquifer to change in groundwater. We rigorously integrate GPS and GRACE in a joint inversion for change in water. In the inversion, GPS strongly constrains water change in California's mountains and GRACE strongly constrains total water change over broad areas. GPS determines water change in the mountains adjacent to the Central Valley; the remaining GRACE water change in the broad region is then assigned by the inversion to be water change in Central Valley. We follow the general strategy of Adusumilli et al. (2019) in that we constrain the total of water change in about 144 quarter-degree pixels to add up to the value in the three-degree GRACE mascon that the pixels lie within. Carlson et al. (2022) also jointly invert GPS and GRACE data in California.

#### 2. Data and Methods

We use (a) GPS positions as a function of time estimated by Nevada Geodetic Laboratory (Blewitt et al., 2018) and (b) GRACE mass changes estimated by NASA's Jet Propulsion Laboratory (Wiese et al., 2016, 2018). We evaluate data from 1937 GPS sites in the western U.S. (Figures S3 and S4 in Supporting Information S1). We carefully perform seven steps to prepare the GPS elastic displacement data: (a) determine monthly mean GPS displacements uninterrupted by offsets due to antenna offsets and earthquakes, (b) remove atmospheric and non-tidal oceanic loading, (c) identify and omit 495 GPS sites recording porous response to groundwater change,

ARGUS ET AL. 3 of 12

influenced by volcanic activity, or biased by postseismic transients, (d) remove elastic displacement created by known changes in surface water in artificial reservoirs, (e) remove glacial isostatic adjustment, (f) remove interseismic strain accumulation created by locking of the Cascadia megathrust, and (g) remove elastic displacement produced by water change outside the western U.S. area that we are solving for.

We simultaneously invert elastic displacements at 1442 GPS sites (Blewitt et al., 2018) and mass changes at 21 three-degree GRACE mascons (Watkins et al., 2015) in the western U.S. GPS and GRACE estimates differ in spatial and temporal resolution. GPS tightly constrains seasonal oscillation and interannual variations across distances less than 110 km where the array is dense in California, Oregon, and Washington. GRACE estimates are accurate across distances of more than 330 km. Tectonic uplift and subsidence and mismodeled glacial isostatic adjustment may bias GPS estimates over many years, whereas GRACE is accurate over decades (e.g., Watkins et al., 2015). By simultaneously inverting GPS and GRACE, we determine optimal estimates of change in total water. We estimate change in total water each month from January 2006 to May 2022 at 6,660 quarter-degree pixels in the region (32°N to 50°N, 125°W to 103°W). We evaluate goodness-of-fit and estimate realistic uncertainties. See Supporting Information S1 for full explanation of Data and Methods.

#### 3. Results

We first evaluate seasonal oscillations and interannual fluctuations in water in the SST River basin, the source watershed of the Central Valley, which includes most of the Sierra Nevada and parts of the California Coast Ranges and southern Cascade and Klamath mountains.

#### 3.1. Change in Water in Sacramento-San Joaquin-Tulare (SST) River Basin

#### 3.1.1. Seasonal Oscillation

The mean peak-to-peak seasonal oscillation in total water in the SST River basin is  $46 \pm 4$  km<sup>3</sup>, consisting of 6 km<sup>3</sup> (13%) of surface water in artificial reservoirs and  $40 \pm 4$  (87%) km<sup>3</sup> of other water (Figures S5 and S6a in Supporting Information S1). We carefully separate change in surface water in artificial reservoirs (recorded by the California Data Exchange Center (CDEC, 2022)) from change in other water following the techniques of Argus et al. (2017, 2020). The rise and fall in total water each year is nearly half the mean annual cumulative precipitation,  $104 \text{ km}^3$ . The mean total seasonal oscillation amounts to an equivalent water thickness of  $0.30 \pm 0.03$  m averaged over the  $154,800 \text{ km}^2$  area of the SST River basin.

Snow accumulation and loss (in SNODAS) in the mountain part of the SST River basin (mostly in the Sierra Nevada) each year produces a rise and fall of 12 km<sup>3</sup> of water, accounting for 26% of the total seasonal oscillation in the SST River basin. However, maximum snowpack varies strongly by year. In heavy precipitation years 2011, 2017, and 2019, snow peaked at a snow water equivalent of, respectively, 28 km<sup>3</sup>, 25 km<sup>3</sup>, and 27 km<sup>3</sup>. In drought years 2014 and 2015, snowpack reached a maximum of just 3 and 2 km<sup>3</sup>.

The seasonal oscillation in total water storage is larger in years of heavy precipitation. In heavy precipitation water years 2011, 2017, and 2019, a total of, respectively, 80, 94, and 82 km<sup>3</sup> of water was gained in the autumn and winter. During drought water years 2012, 2014, and 2021, a total of just 24, 24, and 27 km<sup>3</sup> of water was gained during the wet season. Just a third of the 60 km<sup>3</sup> difference between water gain in the heavy precipitation and the drought years results from differences in snowpack; the remaining two-thirds comes from differences in rainwater and snow infiltrating the ground (cf. Enzminger et al., 2019).

The seasonal oscillation in subsurface water (inferred to be total water minus snow) in the SST River basin is  $30.5 \pm 3.0 \text{ km}^3/\text{yr}$  with a maximum around April 16. This seasonal oscillation in subsurface water is 29% of yearly cumulative precipitation in the basin, 104 km<sup>3</sup>.

The seasonal oscillation in groundwater (inferred to be total water minus snow minus soil moisture) is  $16.8 \pm 1.7 \text{ km}^3/\text{yr}$  with a maximum around July 1. This seasonal oscillation in groundwater is 24% of yearly cumulative precipitation. Maximum groundwater occurs 2.5 months after maximum total water (April 16) in the SST River basin.

ARGUS ET AL. 4 of 12

#### 3.1.2. Rate of Change

The rate of loss of total water in the SST River basin from 2006 to 2021 is  $5.0 \pm 2.5$  km³/yr ( $0.032 \pm 0.016$  m/yr) assuming glacial isostatic adjustment model ICE-6G (VM5a) (Figures S4 and S6b in Supporting Information S1). Assuming instead that solid Earth has entirely relaxed from unloading of the Laurentide ice sheet reduces the estimate of the loss rate to 2.4 km³/yr (right at the 95% bound of the first estimate) and results in better agreement between the GRACE estimate (-3.1 km³/yr) and the GPS estimate (-2.2 km³/yr), suggesting that postglacial viscous relaxation in the western U.S. is nearly complete.

#### 3.1.3. Interannual Variation

We are finding substantial subsurface water, either groundwater or soil moisture (understated by hydrology models), to be lost during periods of drought and gained during years of heavy precipitation (Argus et al., 2017). There is insignificant snow on the ground in the west U.S. at the start of the water year in October. We therefore evaluate changes in subsurface water between successive Octobers.

During moderate drought from October 2006 to October 2009,  $7 \text{ km}^3$  of surface water in artificial reservoirs and  $32 \pm 11 \text{ km}^3$  of soil moisture and groundwater was lost (Figures S5 and S6 in Supporting Information S1). Heavy precipitation in water years 2010 and 2011 replenished all of the surface water and  $24 \pm 9 \text{ km}^3$  (75%) of the subsurface water lost during the prior three drought years.

During harsh drought from October 2011 to October 2015,  $13 \text{ km}^3$  of artificial reservoir surface water and a huge  $95 \pm 10 \text{ km}^3$  of soil moisture and groundwater was lost. This  $95 \text{ km}^3$  decline of subsurface water is six times the  $12 \text{ km}^3$  loss of soil moisture in the (NLDAS) North American Land Data Assimilation–Noah model (Mitchell et al., 2004; Pan et al., 2003). Heavy rain and snow in water years 2016 through 2019 restored most of the surface water and  $48 \pm 11 \text{ km}^3$  (51%) of the subsurface water lost during the prior 4 years of harsh drought. This  $48 \text{ km}^3$  increase in subsurface water is seven times the  $7 \text{ km}^3$  gain in NLDAS-Noah.

During drought from October 2019 to October 2021, 9 km<sup>3</sup> of artificial reservoir surface water and  $48 \pm 9$  km<sup>3</sup> of soil moisture and groundwater was lost. We look forward to calculating water loss through October 2022, the end of the third year of the present drought.

#### 3.2. Change in Water in the Central Valley

Change in water in the Central Valley consists nearly entirely of change in soil moisture and groundwater because snow accumulation is negligible in the Valley. We next infer change in groundwater by assuming soil moisture to be that in the NLDAS–Noah land surface model.

#### 3.2.1. Seasonal Oscillation

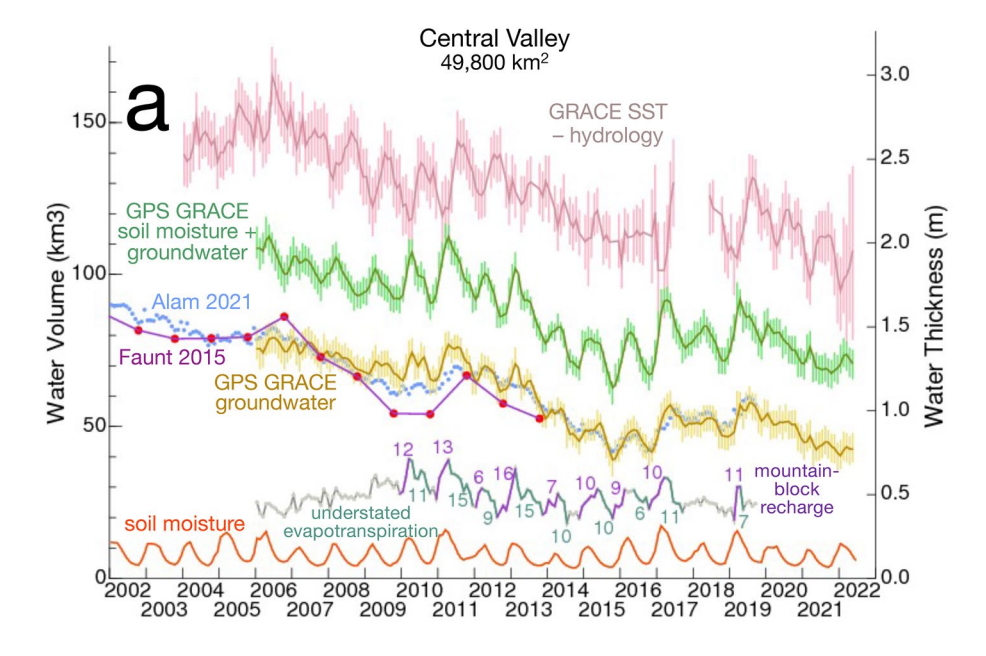
The average seasonal oscillation in total water in the Central Valley is  $10.7 \pm 1.1 \text{ km}^3$  with maximum water storage around April 1 (Figures 2 and 3a). In the wet autumn and winter rain falls into the Valley, raising equivalent water thickness by a mean of  $0.21 \pm 0.02$  m. In the dry spring and summer, water evaporates from the Valley surface and is pumped from the aquifer, reducing equivalent water thickness by on average the same amount. (Values are calculated from the sinusoid fit to estimates of groundwater as a function of time).

We find the seasonal water oscillation to be partitioned between soil moisture  $(7.6 \pm 0.7 \text{ km}^3, \text{ maximum March } 16)$  and groundwater  $(4.9 \pm 0.5 \text{ km}^3, \text{ maximum May } 16)$ . Groundwater is maximum 2 months after soil moisture is maximum. The seasonal oscillation in groundwater is 1.5 times as large as that  $(3.2 \text{ km}^3)$  in the water-balance of Alam et al. (2021), suggesting that there are water cycle processes not accounted for in the balance model (as we describe further in Section 4.1). Perhaps there is a greater capacity for California, under the Sustainable Groundwater Management Act (SGMA) (California State Legislature, 2014), to save groundwater and reduce the long-term rate of Central Valley groundwater depletion.

This study's estimate of the evolution of Central Valley groundwater determined by combining GPS and GRACE is more accurate than that determined using GRACE and assuming a land surface hydrology model by Famiglietti et al. (2011) and subsequent studies. Our realization of the Famiglietti et al. method has a seasonal oscillation in total water of 12 km<sup>3</sup> with maximum around August 16, which is incorrect because water is maximum in the spring. GPS sites recording solid Earth's porous response record subsurface water in the Valley to be maximum

ARGUS ET AL. 5 of 12

19448007, 2022, 22, Downloaded from https://agupubs.onlinelibrary.wiley.com/doi/10.1029/2022GL099888 by University Of Montana Mansfield Library-Serials, Wiley Online Library on [02/12/2022]. See the Terms and Conditions (https://onlinelibrary.wiley



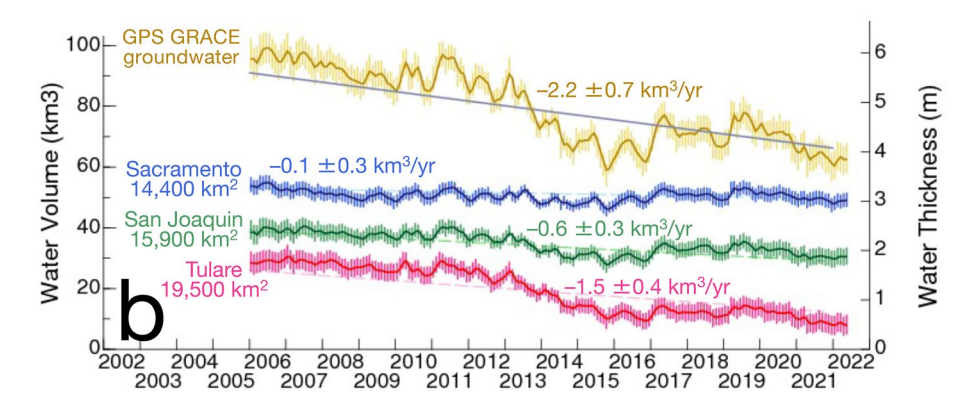
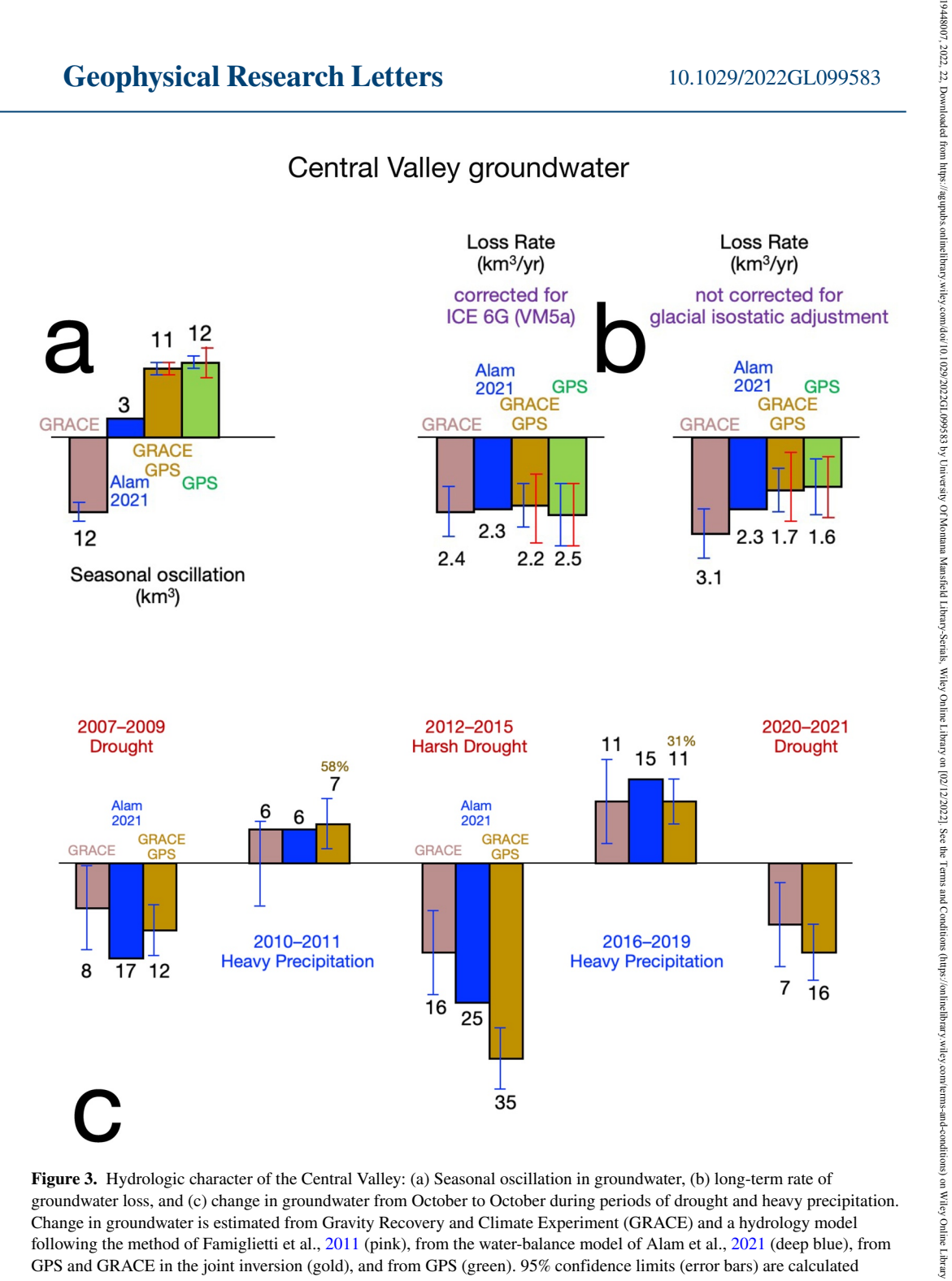


Figure 2. (a) Estimates of change in water in Central Valley from 2002 to 2022: groundwater change estimated using Gravity Recovery and Climate Experiment (GRACE) and the composite hydrology model following the technique of Famiglietti et al. (2011) (pink curve); and groundwater change in this study (gold curve) is equal to change in total water in the GPS/ GRACE joint inversion (green curve) minus change in soil moisture in NLDAS-Noah (orange curve). Error bars are 95% confidence limits. Red circles (connected with violet line segments) are groundwater change in the Central Valley Hydrologic Model (Faunt et al., 2015). Light blue dots are groundwater change in the water balance model of Alam et al. (2021). Estimates of water change are relative not absolute; the curves vertical position on the plot is arbitrary (and chosen to clearly present the estimates). Units of water change are cubic kilometers on the left vertical axis and equivalent water thickess on the right vertical axis. The gray curve (with short violet and short teal green segments) is the difference in groundwater change between the GPS/GRACE/-soil moisture estimate and the Alam et al. (2021) water balance elements and can be attributed to water processes not in the water balance model: violet segments are positive differences inferred to be mountain-block recharge (subsurface flow of groundwater from the mountains to the Valley); and teal green line segments are negative differences inferred to reflect underestimated evapotranspiration associated with groundwater pumping. When we calculate the difference, we remove soil moisture in the Alam et al., 2021 realization of Land Surface Model-VIC (rather than in NLDAS-Noah) to be consistent with the soil moisture model subtracted in that study. The 5.9 km<sup>3</sup> peak-to-peak seasonal oscillation in soil moisture in LSM-VIC is smaller than the 7.6 km3 seasonal oscillation in soil moisture in NLDAS-Noah. (b) Groundwater change in the GPS/GRACE/-soil moisture estimate is partitioned into the northern (Sacramento River part), middle (San Joaquin River), and southern (Tulare River) parts of the Central Valley.

around April 1. A second advantage of our method is that we account for the fact that half of surface water change in artificial reservoirs as observed by GRACE leaks outside of the SST River basin, whereas the Famiglietti et al. method assumes GRACE observes all reservoir water to be inside the SST River basin.

ARGUS ET AL. 6 of 12

# Central Valley groundwater



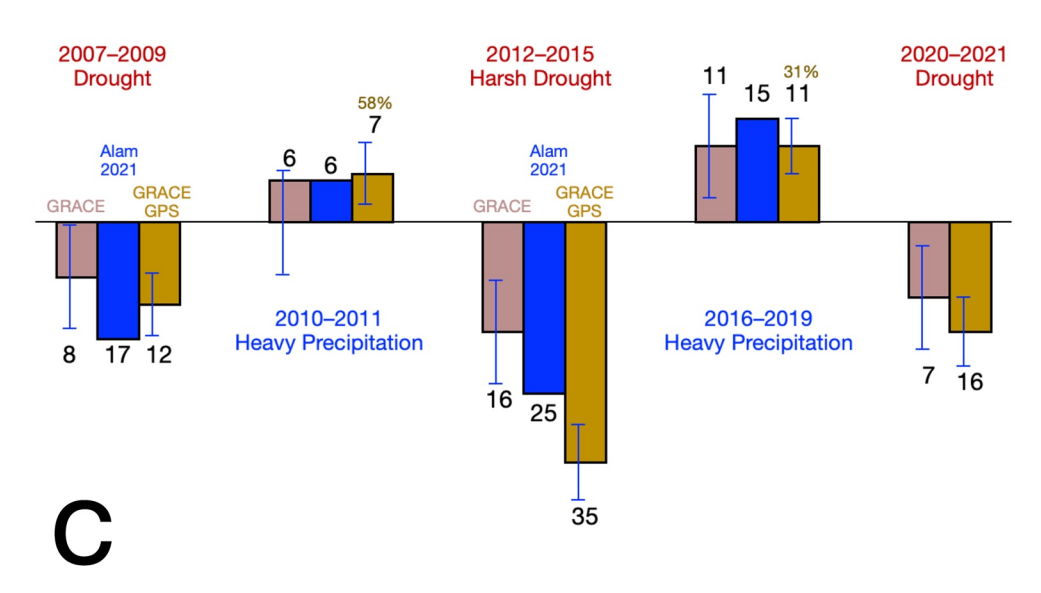


Figure 3. Hydrologic character of the Central Valley: (a) Seasonal oscillation in groundwater, (b) long-term rate of groundwater loss, and (c) change in groundwater from October to October during periods of drought and heavy precipitation. Change in groundwater is estimated from Gravity Recovery and Climate Experiment (GRACE) and a hydrology model following the method of Famiglietti et al., 2011 (pink), from the water-balance model of Alam et al., 2021 (deep blue), from GPS and GRACE in the joint inversion (gold), and from GPS (green). 95% confidence limits (error bars) are calculated using linear propagation of errors (blue) and Hector spectral analysis (red). In (b), the rate of water loss is plotted for estimates correcting for (left) and not correcting for (right) glacial isostatic adjustment model ICE-6G (VM5a) (Argus, Peltier et al., 2014; Peltier et al., 2015, 2018); the estimates are calculated assuming the forebulge of the former Laurentide ice sheet to be presently collapsing in California at respectively, 0.6 mm/yr and 0.0 mm/yr.

#### 3.2.2. Rate of Loss

The Central Valley lost groundwater from 2006 to 2021 at an average rate of  $2.2 \pm 0.7$  km<sup>3</sup>/yr (Figures 2 and 3b) which is  $0.044 \pm 0.14$  m/yr averaged over the  $48,800 \text{ km}^3$  area of the Valley. Our loss rate of  $2.2 \text{ km}^3$ /yr is slower than the 3.1 km<sup>3</sup>/yr rate from 2003 to 2010 estimated by Famiglietti et al. (2011) but comparable to the 1.7 km<sup>3</sup>/ yr rate from 1960 to 2011 estimated from hydrologic data (Faunt, 2009).

ARGUS ET AL. 7 of 12 By integrating GPS and GRACE, we resolve the spatial distribution of groundwater loss across the Central Valley. The northern, central, and southern Central Valley lost water from 2006 to 2021 at average rates of, respectively,  $0.1 \pm 0.3 \text{ km}^3/\text{yr}$ ,  $0.6 \pm 0.3 \text{ km}^3/\text{yr}$ , and  $1.5 \pm 0.4 \text{ km}^3/\text{yr}$ . The southern Valley lost  $24 \pm 4 \text{ km}^3$  of groundwater from 2006 to 2021, reducing equivalent water thickness by  $0.48 \pm 0.08 \text{ m}$ . The result that the southern Central Valley is losing groundwater most rapidly is consistent with the spectacular rates of subsidence observed in parts of Tulare basin (Farr & Liu, 2014; Neely et al., 2021; Ojha et al., 2018, 2019) (Figure 1).

#### 3.2.3. Interannual Variation

Groundwater in the Central Valley is lost during periods of drought and gained during periods of heavy precipitation (Figures 2 and 3c). During moderate drought from October 2006 to October 2009, the Central Valley lost  $12 \pm 4 \text{ km}^3$  of groundwater. Heavy precipitation in water years 2006 through 2009 restored  $7 \pm 4 \text{ km}^3$  of groundwater, 58% of the loss during the prior three years.

During harsh drought from October 2011 to October 2015, the Central Valley lost  $35 \pm 4$  km<sup>3</sup> of groundwater, reducing equivalent water thickness by  $0.70 \pm 0.08$  m. If the mean rock porosity of the Central Valley were 0.2, then groundwater well levels would have fallen by a mean of 3.5 m. Heavy precipitation from water years 2016 through 2019 replenished  $11 \pm 4$  km<sup>3</sup> of groundwater, 31% of the loss during the four harsh drought years.

Our estimates of recharge of Central Valley groundwater from GPS and GRACE are 58% (2006–2011) and 31% (2012–2019). The latter 31% recharge is less than the 60% recharge estimated from a water-balance model by Alam et al. (2021).

#### 4. Inference

#### 4.1. Inferring Mountain-Block Recharge and Evapotranspiration of Pumped Groundwater

In their water-balance model, Alam et al. (2021) estimate change in total groundwater in the Central Valley by accounting for all water processes bringing water into and taking water out of the Valley:

$$\Delta S = P + Q_{in} - Q_{out} - E \tag{2}$$

$$\Delta S = \Delta_{\text{snow}} + \Delta_{\text{soil moisture}} + \Delta_{\text{surface water}} + \Delta_{\text{groundwater}}$$
(3)

where  $\Delta S$  is change in total water in the Central Valley, P is precipitation, E is evapotranspiration,  $Q_{\rm in}$  is surface water entering the Valley along 52 rivers and creeks from the surrounding mountains, and  $Q_{\rm out}$  is surface water leaving the Valley at the Sacramento-San Joaquin River Delta.

Eliminating  $\Delta S$ , Alam et al. find:

$$\Delta_{\text{groundwater}} = P + Q_{in} - Q_{out} - E - \Delta_{\text{snow}} - \Delta_{\text{soil moisture}} - \Delta_{\text{surface water}}$$
(4)

 $Q_{\rm in}$  and  $Q_{\rm out}$  are from river gauges (CDWR, 2020; USGS, 2020); precipitation is from PRISM (Daly et al., 2008); evapotranspiration and soil moisture are from the LSM-VIC model of Alam et al. (2021); artificial reservoir surface water is from CDEC (2022); snow accumulation is from SNODAS (NOHRSC, 2004).

Differences between our and Alam et al.'s (2021) estimate of Central Valley groundwater reflect groundwater fluctuations observed by GPS and GRACE but not accounted for by Alam et al. (2021), as well as uncertainties in the measurements and inversion. Positive differences reflect increases in groundwater arising from mountain-block recharge, which is subsurface flow of groundwater from the mountains (mostly Sierra Nevada, also southern Cascade and Klamath mountains and Coast Ranges) into the Central Valley (Figure 2a, violet segments). Negative differences may reflect evapotranspiration of pumped groundwater that are underestimated by the water-balance model (Figure 2a, yellow segments). Subsurface recharge occurs in autumn and winter and tends to be larger in heavy precipitation years (13, 10, and 11 km³ in, respectively, water years 2011, 2017, and 2019). Evapotranspiration during spring and summer is understated by the Alam et al. water-balance model by on average 8 km³ from 2010 to 2019.

A total of 50 km<sup>3</sup> of water recharges the Central Valley each year, consisting of 28 km<sup>3</sup> from rivers, 17 km<sup>3</sup> from precipitation, and 5 km<sup>3</sup> from subsurface flow of groundwater from the mountains to the Valley (mountain-block recharge). The 24 km<sup>3</sup> of river water each year leaving the Central Valley at Sacramento-San Joaquin Delta is 87%

ARGUS ET AL. 8 of 12

of the 28 km<sup>3</sup> of river water entering the Valley from the SST watershed. The inferred 4.8 km<sup>3</sup> of groundwater moving in the deep subsurface from the mountains to the Central Valley is comparable to the 4.2 km<sup>3</sup> of net river inflow and 1/4 of yearly rainfall. Therefore mountain-block recharge plays an essential role in replenishment of Central Valley groundwater.

Using GPS and InSAR measurements of vertical displacements of the southern Central Valley's surface, and taking such displacements to reflect the aquifer's porous response, Neely et al. (2021) infer the timing and magnitude of changes in groundwater in the Tulare River basin part of the Valley in water years 2016 and 2017. Our estimates of the evolution of groundwater in the southern Tulare part of the Central Valley (Figure 2b, red violet curve) provide constraints complementary to Neely et al.'s detailed inferences on how the change in groundwater varies across the aquifer.

#### 5. Conclusions

In this study, we first determine change in total water at Earth's surface using GPS elastic displacements and GRACE gravity data. We next remove snow water equivalent to estimate change in subsurface water. We then remove soil moisture to infer estimates of groundwater change. We ultimately take differences between our estimate of Central Valley groundwater change and that in a water-balance model to be phenomena not included in the model. We are finding constructive conclusions concerning the water cycle:

- 1. In the SST River basin, the seasonal oscillation in subsurface water (soil moisture plus groundwater),  $30.5 \pm 3.0 \text{ km}^3$ , is 29% of the mean cumulative precipitation,  $104 \text{ km}^3$ .
- 2. From 2006 to 2021, the Central Valley lost groundwater at a rate of 2.2 km<sup>3</sup>/yr, with 68% of the loss being from the southern (Tulare) part of the Valley.
- 3. In the Central Valley, the seasonal oscillation in subsurface water is  $10.7 \pm 1.1 \text{ km}^3$ , with maximum water around April 1 (not in August as inferred from GRACE data).
- 4. The seasonal oscillation in groundwater in the Central Valley is 4.9 ± 0.5 km<sup>3</sup>, with maximum groundwater around May 16. Groundwater is maximum in the Central Valley two months after snow in the SST River basin (mostly in the Sierra Nevada) is maximum around March 16.
- 5. Our GRACE/GPS estimate of change in Central Valley groundwater agrees to a high degree with that from the water-balance model of Alam et al., 2021, in particular in long-term rate of loss and interannual fluctuations. Differences in seasonal oscillation between the two estimates reflect processes not accounted for in the water-balance model. An average of 5 km³ of groundwater each year are inferred to flow in autumn and winter in the deep subsurface from the mountains to the Central Valley. Evapotranspiration in the spring and summer is underestimated in the water-balance model by 5 km³ and likely results from groundwater pumping.
- 6. Of the 50 km³ of water entering the Central Valley each year, 28 km³ comes from rivers, 17 km³ from precipitation, and 5 km³ from mountain groundwater.

#### **Data Availability Statement**

This study's estimates of total water storage inferred from GPS and GRACE as a function of location each month from January 2006 to May 2022 are publicly available at https://zenodo.org/record/7105955#.Y0CMAezMI74. JPL's GRACE Mascon solution is available at https://grace.jpl.nasa.gov/data/get-data/jpl\_global\_mascons/. Nevada Geodetic Laboratory series of GPS postions as a function of time are available at http://geodesy.unr.edu/gps\_timeseries/tenv3/IGS14/.

## References

Adusumilli, S., Fish, A. M. A., Fish, M. A., McMillan, H. K., & Silverii, F. (2019). A decade of water storage changes across the contiguous United States from GPS and satellite gravity. *Geophysical Research Letters*, 46(22), 13006–13015. https://doi.org/10.1029/2019GL085370 Ahamed, A., Knight, R., Alam, S., Pauloo, R., & Melton, F. (2022). Assessing the utility of remote sensing data to accurately estimate changes in groundwater storage. *Science of the Total Environement*, 807, 150635. https://doi.org/10.1016/j.scitotenv.2021.150635

Alam, S., Gebremichael, M., Ban, Z., Scanlon, B. R., Senay, G., & Lettenmaier, D. P. (2021). Post-drought groundwater storage recovery in California's the Central Valley. Water Resources Research, 57(10), e2021WR030352. https://doi.org/10.1029/2021WR030352

Argus, D. F., Fu, Y., & Landerer, F. W. (2014a). Seasonal variation in total water storage in California inferred from GPS observations of vertical land motion. *Geophysical Research Letters*, 41(6), 1971–1980. https://doi.org/10.1002/2014GL059570

#### Acknowledgments

The authors are grateful to Geoff Blewitt, Corne Kreemer, and Bill Hammond for making GPS positions publicly available; to Paul Ries, Mike Heflin, and Willy Bertiger and others on Jet Propulsion Laboratory's GPS geodesy team for making GPS satellite orbits and clocks and the GipsyX software publicly available; to Dennis Lettenmaier for knowledge on land surface hydrology models; to Jean-Philippe Avouac, Kristel Chanard, and Stacy Larochelle for constructive feedback on distinguishing between phenomena deforming solid Earth; and to Yuanjin Pan and an anonymous reviewer for constructive feedback. This research was supported by grants NASA NNH18ZDA001N-ESI NASA, NASA NNH19ZDA001N-ESI, and National Science Foundation 2021637. Part of this research was performed at Jet Propulsion Laboratory, California Institute of Technology, under NASA contract.

ARGUS ET AL. 9 of 12

19448007, 2022,

- Argus, D. F., Landerer, F. W., Wiese, D. N., Martens, H. R., Fu, Y., Famiglietti, J. S., et al. (2017). Sustained water loss in California's mountain ranges during severe drought from 2012 to 2015 inferred from GPS. *Journal of Geophysical Research: Solid Earth*, 122(12), 10559–10585. https://doi.org/10.1002/2017JB014424
- Argus, D. F., Peltier, W. R., Drummond, R., & Moore, A. W. (2014b). The Antarctica component of postglacial rebound model ICE-6G\_C (VM5a) based on GPS positioning, exposure age dating of ice thicknesses, and relative sea level histories. *Geophysical Journal International*, 198(1), 537–563. https://doi.org/10.1093/gji/ggu140
- Argus, D. F., Ratliff, B., DeMets, C., Borsa, A. A., Wiese, D. N., Blewitt, G., et al. (2020). Rise of great lakes surface water, sinking of the upper Midwest of the United States, and viscous collapse of the forebulge of the former laurentide ice sheet. *Journal of Geophysical Research: Solid Earth*, 125(9), e2020JB019739. https://doi.org/10.1029/2020JB019739
- Blewitt, G., Hammond, W. C., & Kreemer, C. (2018). Harnessing the GPS data explosion for interdisciplinary science. *Eos*, 99. https://doi.org/10.1029/2018EO104623
- Borsa, A. A., Agnew, D. C., & Cayan, D. R. (2014). Ongoing drought-induced uplift of the Western United States. *Science*, 345(6204), 1587–1590. https://doi.org/10.1126/science.1260279
- California Department of Water Resources. (2018). Hydroclimate Report water year 2017. California. Retrieved from https://water.ca.gov/climate-meteorology
- California Department of Water Resources. (2020). C2VSimFG version 1.0: Fine grid California Central Valley groundwater-surface water simulation model. Retrieved from https://data.cnra.ca.gov/dataset/c2vsimfg-version-1-0
- California Department of Water Resources. (2022). Retrieved from https://cdec.water.ca.gov/reservoir.html
- California State Legislature. (2014). Sustainable groundwater management act. Retrieved from https://www.opr.ca.gov/docs/2014\_Sustainable\_ Groundwater Management Legislation 092914.pdf
- Carlson, G., Werth, S., & Shirzaei, M. (2022). Joint inversion of GNSS and GRACE for terrestrial water storage change in California. *Journal of Geophysical Research: Solid Earth*, 127(3), e2021JB023135. https://doi.org/10.1029/2021JB023135
- Cayan, D. R., Redmond, K. T., & Riddle, L. (1999). ENSO and hydrologic extremes in the Western United States. *Journal of Climate*, 12(9), 2881–2893. https://doi.org/10.1175/1520-0442(1999)012<2881;EAHEIT>2.0.CO;2
- Daly, C., Halbleib, M., Smith, J. I., Gibson, W. P., Doggett, M. K., Taylor, G. H., et al. (2008). Physiographically sensitive mapping of climatological temperature and precipitation across the conterminous United States. *International Journal of Climatology*, 28(15), 2031–2064. https://doi.org/10.1002/joc.1688
- Enzminger, T. L., Small, E. E., & Borsa, A. A. (2019). Subsurface water dominates Sierra Nevada seasonal hydrologic storage. Geophysical Research Letters, 46(21), 11993–12001. https://doi.org/10.1029/2019GL084589
- Famiglietti, J. S., Lo, M., Ho, S. L., Bethune, J., Anderson, K. J., Syed, T. H., et al. (2011). Satellites measure recent rates of groundwater depletion in California's the Central Valley. *Geophysical Research Letters*, 38(3), L03403. https://doi.org/10.1029/2010GL046442
- Farr, T. G., & Liu, Z. (2014). Monitoring subsidence associated with groundwater dynamics in the Central Valley of California using interferometric radar. In V. Lakshmi, et al. (Eds.), Remote sensing of the terrestrial water cycle (pp. 397–406). John Wiley, Inc. https://doi.org/10.1002/9781118872086.ch24
- Faunt, C. C. (2009). Groundwater availability of the Central Valley aquifer, California. U.S. Geological Survey professional paper 1766.
- Faunt, C. C., Sneed, M., Traum, J., & Brandt, J. T. (2015). Water availability and land subsidence in the Central Valley, California, USA. *Hydrogeology Journal*, 24(3), 675–684. https://doi.org/10.1007/s10040-015-1339-x
- Griffin, D., & Anchukaitis, K. J. (2014). How unusual is the 2012–2014 California drought? Geophysical Research Letters, 41(24), 9017–9023. https://doi.org/10.1002/2014GL062433
- Intergovernmental Panel on Climate Change. (2021). Climate Change 2021: The physical scientific basis. In V.Masson-Delmotte, P. Zhai, A. Pirani, S. L. Connors, C. Péan, S. Berger, et al. (Eds.), Contribution of working Group 1 to the sixth assessment report on the intergovernmental panel on climate change, 3949 pp.Cambridge University Press. Retrieved from https://www.ipcc.ch/2021/08/09/ar6-wg1-20210809-pr/
- Kim, K. H., Liu, Z., Rodell, M., Beaudoing, H., Massoud, E., Kitchens, J., et al. (2020). An evaluation of remotely sensed and in situ data sufficiency for SGMA-scale groundwater studies in the Central Valley, California. *Journal of the American Water Resources Association*, 57(5), 1–11. https://doi.org/10.1111/1752-1688.12898
- Landerer, F. W., Flechtner, F. M., Save, H., Webb, F. H., Bandikova, T., Bertiger, W. I., et al. (2020). Extending the global mass change data record: GRACE follow-on instrument and science data performance. Geophysical Research Letters, 47(12), e2020GL088306. https://doi.org/10.1029/2020GL088306
- Liu, Z., Liu, P. W., Massoud, E., Farr, T. G., Lundgren, P., & Famiglietti, J. S. (2019). Monitoring groundwater change in California's Central Valley using Sentinel-1 and GRACE observations. *Geosciences*, 9(10), 436. https://doi.org/10.3390/geosciences9100436
- Mitchell, K. E., Lohmann, D., Houser, P. R., Wood, E. F., Schaake, J. C., Robock, A., et al. (2004). The multi-institution North American Land Data Assimilation System (NLDAS): Utilizing multiple GCIP products and partners in a continental distributed hydrological modeling system. *Journal of Geophysical Research*, 109(D7), D07S90. https://doi.org/10.1029/2003JD003823
- National Operational Hydrologic Remote Sensing Center. (2004). Snow data assimilation system (SNODAS) data products at NSIDC, version 1. National snow and ice data center. NSIDC: National Snow and Ice Data Center. https://doi.org/10.7265/N5TB14TC
- Neely, W. R., Borsa, A. A., Burney, J. A., Levy, M. C., Silverii, F., & Sneed, M. (2021). Characterization of groundwater recharge and flow in California's San Joaquin Valley from InSAR-observed surface deformation. Water Resources Research, 57(4), e2020WR028451. https://doi. org/10.1029/2020WR028451
- Ojha, C., Shirzaei, M., Werth, S., Argus, D. F., & Farr, T. G. (2018). Sustained groundwater loss in California's the Central Valley exacerbated by intense drought periods. Water Resources Research, 54(7), 4449–4460. https://doi.org/10.1029/2017WR022250
- Ojha, C., Werth, S., & Shirzaei, M. (2019). Groundwater loss and aquifer system compaction in San Joaquin Valley during 2012–2015 drought. Journal of Geophysical Research: Solid Earth, 124(3), 3127–3143. https://doi.org/10.1029/2018JB016083
- Pan, M., Sheffield, J., Wood, E. F., Mitchell, K. E., Houser, P. R., Schaake, J. C., et al. (2003). Snow process modeling in the north American land data assimilation system (NLDAS): 2. Evaluation of model simulated snow water equivalent. *Journal of Geophysical Research*, 108(D22), 8850. https://doi.org/10.1029/2003JD003994
- Peltier, W. R., Argus, D. F., & Drummond, R. (2015). Space geodesy constrains ice age terminal deglaciation: The global ICE-6G\_C (VM5a) model. *Journal of Geophysical Research: Solid Earth*, 120(1), 450–487. https://doi.org/10.1002/2014JB011176
- Peltier, W. R., Argus, D. F., & Drummond, R. (2018). Comment on the paper by Purcell et al. 2016 entitled 'An assessment of ICE-6G\_C (VM5a) glacial isostatic adjustment model. *Journal of Geophysical Research: Solid Earth*, 122. https://doi.org/10.1002/2016JB013844
- PRISM Climate Group. (2017). Northwest alliance for computation science and engineering. Oregon State University. Retrieved from <a href="http://www.prism.oregonstate.edu/">http://www.prism.oregonstate.edu/</a>

ARGUS ET AL. 10 of 12

19448007, 2022,

- Rodell, M., Houser, P. R., Jambor, U., Gottschalck, J., Mitchell, K., Meng, C. J., et al. (2004). The global land data assimilation system. *Bulletin of the American Meteorological Society*, 85(3), 381–394. https://doi.org/10.1175/BAMS-85-3-381
- Scanlon, B. R., Faunt, C. C., Longuevergne, L., Reedy, R. C., Alley, W. M., McGuire, V. L., & McMahon, P. B. (2012). Groundwater depletion and sustainability of irrigation in the U.S. high Plaines and Central Valley. *Proceedings of the National Academy of Sciences*, 109(24), 9320–9325. https://doi.org/10.1073/pnas.1200311109
- Swain, D. L., Tsiang, M., Haugen, M., Singh, D., Charland, A., Rajaratnam, B., & Diffenbaugh, N. S. (2014). The extraordinary California drought of 2013/2014: Character, context, and the role of climate change. *Bulletin of the American Meteorological Society*, 95, S3–S7.
- Thelin, G. P., & Pike, R. J. (1991). Landforms of the conterminous United States—a digital shaded-relief portrayal, U.S. Dept. Interior.
- U.S. Drought Monitor. (2021). U.S. Drought monitor update for december 21, 2021. Retrieved from https://www.ncei.noaa.gov/news/us-drought-monitor-update-december-21-2021
- USGS. (2020). USGS water data for the nation, U.S. Geological Survey National Water Information System database available on the world wide web (USGS water data for the nation). https://doi.org/10.5066/F7P55KJN
- Watkins, M. M., Wiese, D. N., Yuan, D.-N., Boening, C., & Landerer, F. W. (2015). Improved methods for observing Earth's time variable mass distribution with GRACE using spherical cap mascons. *Journal of Geophysical Research: Solid Earth*, 120(4), 2648–2671. https://doi.org/10.1002/2014JB011547
- Wiese, D. N., Landerer, F. W., & Watkins, M. M. (2016). Quantifying and reducing leakage errors in the JPL RL05M GRACE Mascon solution. Water Resources Research, 52(9), 7490–7502. https://doi.org/10.1002/2016WR019344
- Wiese, D. N., Yuan, D.-N., Boening, C., Landerer, F. W., & Watkins, M. M. (2018). JPL GRACE mascon ocean, ice, and hydrology equivalent water height release 06 coastal resolution improvement (CRI) filtered version 1.0. https://doi.org/10.5067/TEMSC-3MJC6

## **References From the Supporting Information**

- Agnew, D. C. (2012). SPOTL: Some programs for ocean-tide loading. Scripps institute of oceanography. Retrieved from https://escholarship.org/uc/item/954322pg
- Argus, D. F., Gordon, R. G., Heflin, M. B., Ma, C., Eanes, R. J., Willis, P., et al. (2010). The angular velocities of the plates and the velocity of Earth's center from space geodesy. *Geophysical Journal International*, 180(3), 913–960. https://doi.org/10.1111/j.1365-246X.2009.04463.x
- Argus, D. F., & Peltier, W. R. (2010). Constraining models of postglacial rebound using space geodesy: A detailed assessment of model ICE-5G (VM2) and its relatives. *Geophysical Journal International*, 181. https://doi.org/10.1111/j.1365-246X.2010.04562.x
- Argus, D. F., Peltier, W. R., Blewitt, G., & Kreemer, C. (2021). The viscosity of the top third of the lower mantle estimated using GPS, GRACE, and relative sea level measurements of glacial isostatic adjustment. *Journal of Geophysical Research: Solid Earth*, 126(5). https://doi.org/10.1029/2020Jb021537
- Bertiger, W., Bar-Sever, Y., Dorsey, A., Haines, B., Harvey, N., Hemberger, D., et al. (2020). GipsyX/RTGx, a new tool set for space geodetic operations and research. *Advances in Space Research*, 66(3), 469–489. https://doi.org/10.1016/j.asr.2020.04.015
- Bevington, P. R., & Robinson, D. K. (2003). Data reduction and error analysis for the physical sciences (third edition). The MCGRAW-Hill
- Boehm, J., Werl, B., & Schuh, H. (2006). Troposphere mapping functions for GPS and very long baseline interferometry from European Centre for Medium-Range Weather Forecasts operational analysis data. *Journal of Geophysical Research*, 111(B02406), 1–9. https://doi.org/10.1029/2005JB003629
- Boehm, J., Werl, B., & Schuh, H. (2007). A global model of pressure and temperature for geodetic applications. *Journal of Geophysical Research*, 111. B02406. https://doi.org/10.1097/s00190-007-0135-3
- Bos, M. S., Fernandes, R. M. S., Williams, S. D. P., & Bastos, L. (2013). Fast error analysis of continuous GNSS observations with missing data. Journal of Geodesy, 87(4), 351–360. https://doi.org/10.1007/s00190-012-0605-0
- Chanard, K., Avouac, J. P., Ramillien, G., & Genrich, J. (2014). Modeling deformation induced by seasonal variations of continental water in the Himalaya region: Sensitivity to Earth elastic structure. *Journal of Geophysical Research: Solid Earth*, 119(6), 5097–5113. https://doi. org/10.1002/2013JB010451
- Chanard, K., Fleitout, L., Calais, E., Rebischung, P., & Avouac, J.-P. (2018). Toward a global horizontal and vertical elastic load deformation model derived from GRACE and GNSS station position time series. *Journal of Geophysical Research: Solid Earth*, 123(4), 3225–3237. https://doi.org/10.1002/2017JB015245
- D'Urso, M. G., & Marmo, F. (2013). On a generalized Love's problem. Computers & Geosciences, 61, 144–151. https://doi.org/10.1016/j.cageo.2013.09.002
- Dill, R., & Dobslaw, H. (2013). Numerical simulations of global-scale high resolution hydrological crustal deformations. *Journal of Geophysical Research: Solid Earth*, 118(9), 5008–5017. https://doi.org/10.1002/jgrb.50353
- Dziewonski, A. M., & Anderson, D. L. (1981). Preliminary reference Earth model. *Physics of the Earth and Planetary Interiors*, 25(4), 297–356. https://doi.org/10.1016/0031-9201(81)90046-7
- Farrell, W. E. (1972). Deformation of the Earth by surface loads. Reviews of Geophysics, 10(3), 761–797. https://doi.org/10.1029/RG010i003p00761
  Fu, Y., Argus, D. F., & Landerer, F. W. (2015). Seasonal and interannual variations of water storage in Washington and Oregon estimated from GPS measured surface loading deformation. Journal of Geophysical Research: Solid Earth, 120(1), 552–566. https://doi.org/10.1002/2014JB011415
- Heflin, M., Donnellan, A., Parker, J., Lyzenga, G., Moore, A., Ludwig, L. G., et al. (2020). Automated estimation and tools to extract positions, velocities, breaks, and seasonal terms from daily GNSS measurements: Illuminating nonlinear Salton trough deformation. Earth and Space Science, 7, e2019EA000644. https://doi.org/10.1029/2019EA000644
- Hyndman, R. D., & Currie, C. A. (2011). Whys it the North America cordillera high? Hot backarcs, thermal isostacy, and mountain belts. *Geology*, 39(8), 783–786. https://doi.org/10.1130/G31998.1
- Jaeger, J. C., Cook, N. G. W., & Zimmerman, R. (2007). Fundamentals of rock mechanics (4th ed.). Wiley-Blackwell.
- Jin, Z., & Fialko, Y. (2020). Finite slip models of the 2019 Ridgecrest earthquake sequence constrained by space geodetic data and aftershock locations. Bulletin of the Seismological Society of America, 110(4), 1660–1679. https://doi.org/10.1785/0120200060
- Kreemer, C., Hammond, W. C., & Blewitt, G. (2018). A robust estimation of the 3-D intraplate deformation of the North American plate from GPS. Journal of Geophysical Research: Solid Earth, 123(5), 4388–4412. https://doi.org/10.1029/2017JB015257
- Kusche, J., & Schrama, E. J. O. (2005). Surface mass redistribution inversion from global GPS deformation and Gravity Recovery and Climate Experiment (GRACE) gravity data. *Journal of Geophysical Research*, 110(B9), B09409. https://doi.org/10.1029/2004JB003556
- Leonard, L. J., Currie, C. A., Mazzotti, S., & Hyndman, R. D. (2010). Rupture area and displacement of past Cascadia great earthquakes from coastal coseismic subsidence. The Geological Society of America Bulletin, 122(11/12), 2079–2096. https://doi.org/10.1130/B30108.1

ARGUS ET AL.

- Li, S., Wang, K., Wang, Y., Jiang, Y., & Dosso, S. E. (2018). Geodetically inferred locking state of the Cascadia megathrust based on a viscoelastic Earth model. *Journal of Geophysical Research: Solid Earth*, 123(9), 8056–8072. https://doi.org/10.1029/2018JB015620
- Martens, H. R., Argus, D. F., Norberg, C., Blewitt, G., Herring, T. A., Moore, A. W., et al. (2020). Atmospheric pressure loading in GPS positions: Dependency on GPS processing methods and effect on assessment of seasonal deformation in the contiguous USA and Alaska. *Journal of Geodynamics*, 94(12), 115. https://doi.org/10.1007/s00190-020-01445-w
- Martens, H. R., Rivera, L., & Simons, M. (2019). LoadDef: A python-based toolkit to model elastic deformation caused by surface mass loading on spherically symmetric bodies. Earth and Space Science, 6(2), 311–323. https://doi.org/10.1029/2018EA000462
- Montgomery-Brown, E. K., Wicks, C. W., Cervelli, P. F., Langbein, J. O., Svarc, J. L., Shelly, D. R., et al. (2015). Renewed inflation of long valley Caldera, California (2011 to 2014). Geophysical Research Letters, 42(13), 5250–5257. https://doi.org/10.1002/2015GL064338
- Murray, K. D., & Lohman, R. B. (2018). Short-lived pause in Central California subsidence after heavy winter precipitation of 2017. Science Advances, 4(8), eaar8144. https://doi.org/10.1126/sciadv.aar8144
- Petit, G., & Luzum, B. (2010). IERS technical note 36 (p. 179). Bundesamts für Kartogr. und Geod.
- Simmons, A., Uppala, S., Dee, D., & Kobayashi, S. (2007). ERA-interim: New ECMWF reanalysis products from 1989 onwards. ECMWF Newsletter, 110, 25–35.
- Sun, Y., Ditmar, P., & Riva, R. (2017). Statistically optimal estimation of degree-1 and C<sub>20</sub> coefficients based on GRACE data and an ocean bottom pressure model. *Geophysical Journal International*, 210(3), 1305–1322. https://doi.org/10.1093/gji/ggx241
- Tellinghuisen, J. (2001). Statistical error propagation. *Journal of Physical Chemistry A*, 105(15), 3917–3921. https://doi.org/10.1021/jp003484u Tregoning, P., & Herring, T. (2006). Impact of a priori zenith hydrostatic delay errors on GPS estimates of station heights and zenith total delays. *Geophysical Research Letters*, 33(23), L23303. https://doi.org/10.1029/2006gl027706
- Wahr, J., Khan, S. A., van Dam, T., Liu, L., van Angelen, J. H., van den Broeke, M. R., & Meertens, C. M. (2013). The use of GPS horizontals for loading studies, with applications to northern California and southeast Greenland. *Journal of Geophysical Research: Solid Earth*, 118, 1795–1806. https://doi.org/10.1002/jgrb.50104
- Wang, H., Xiang, L., Jia, L., Jiang, L., Wang, Z., Hu, B., & Gao, P. (2012). Load Love numbers and Green's functions for elastic Earth models PREM, iasp91, ak135, and modified models with refined crustal structure from crust 2.0. Computational Geosciences, 49, 190–199. https://doi.org/10.1016/j.cageo.2012.06.022
- Wei, S., Fielding, E., Leprince, S., Salden, A., Avouac, J.-P., Helmberger, D., et al. (2011). Superficial simplicity of the 2010 El Mayor–cucapah earthquake of baja California in Mexico. *Nature Geoscience*, 4(9), 615–618. https://doi.org/10.1038/ngeo1213
- Williams, S. D. P. (2008). CATS: GPS coordinate time series analysis software. GPS Solutions, 12(2), 147–153. https://doi.org/10.1007/s10291-007-0086-4
- Young, Z. M., Kreemer, C., & Blewitt, G. (2021). GPS constraints on drought-induced groundwater loss around Great Salt Lake, Utah, with implications for seismicity modulation. *Journal of Geophysical Research: Solid Earth*, 126(10), e2021JB022020. https://doi.org/10.1029/2021JB022020

ARGUS ET AL. 12 of 12